Spectrochimica Acta Part A: Molecular and Biomolecular Spectroscopy 247 (2021) 119077

Contents lists available at ScienceDirect

Spectrochimica Acta Part A: Molecular and Biomolecular Spectroscopy

journal homepage: www.elsevier.com/locate/saa

# Characterization of glycated hemoglobin based on Raman spectroscopy and artificial neural networks

N. González-Viveros [a,*], J. Castro-Ramos [a], P. Gómez-Gil [a], H.H. Cerecedo-Núñez [b]

[a] National Institute of Astrophysics, Optics and Electronics, Luis Enrique Erro No. 1, Santa María Tonantzintla, San Andrés Cholula, C.P. 72840 Puebla, México
[b] Faculty of Physics, Veracruzan University, Zona Universitaria, C.P. 91090 Xalapa, Veracruz, México

ARTICLE INFO

*Article history:*
Received 24 July 2020
Received in revised form 1 October 2020
Accepted 9 October 2020
Available online 21 October 2020

*Keywords:*
Glycated hemoglobin (HbA1c)
Raman spectroscopy
Artificial neural networks (ANN)

ABSTRACT

The World Health Organization has declared the glycated hemoglobin (HbA1c) as a gold standard biomarker for diabetes diagnosis; this has led to relevant research on the spectral behavior and characterization of HbA1c. This paper presents an analysis of Raman peaks of commercial lyophilized HbA1c, diluted in distilled water, using concentrations of 4.76% and 9.09%, as well as pure powder (100% concentration). Vibrational Raman peak positions of HbA1c powder were found at 1578, 1571, 1536, 1436, 1311, 1308, 1230, 1222, 1114, 1106, 969, 799 and 665 $cm^{-1}$; these values are consistent with results reported in other works. Besides, a nonlinear regression model based on a Feed-Forward Neural Network (FFNN) was built to quantify percentages of HbA1c for unknown concentrations. Using the Raman spectra as independent variables, the regression provided a Root Mean Square Error in Cross-Validation (RMSECV) of 0.08% ± 0.04. We also include a detailed molecular assignment of the average spectra of lyophilized powder of HbA1c.



## 1. Introduction

The American Diabetes Association and other related organizations world- wide have recommended the measure of glycated hemoglobin (HbA1c) to aid in diabetes diagnosis. This test consists of analyzing patients' blood samples; therefore, it is an invasive technique. The percentage of HbA1c shows a cumulative glycemic history of the patient over the last two to three months [1–4]. HbA1c is formed by nonenzymatic glycosylation of hemoglobin exposed to blood glucose. During this reaction, the glucose condensed with the N-amino group of a $\beta$ chain of hemoglobin, specifically the amino acid valine, forms a weakly stable ketoamine called Schiff's base. Subsequently, the ketoamine bond, also known as Pre-A1c, results in a modification called the Amadori rearrangement, producing a stable ketoamine bond, which results in HbA1c [5]. Fig. 1 shows the formation scheme and formula of HbA1c.

HbA1c detection is of great importance; consequently, several methods have been proposed for its analysis and measurement, such as immunoassay [7–9], high-pressure liquid chromatography [10,11], spectrophotometry [12–14], ion-exchange and affinity chromatography [15–18], among others. Most of such methods used for HbA1c detection are based on the chemical rupture of hemoglobin fractions, both not glycated and glycated hemoglobin [19].

In the last years, several optical approaches have been reported for characterization, identification, and quantification of HbA1c [20,21]. For instance, the work published in [22] used different concentrations of lyophilized human red blood cells and applied a linear regression supported by the area under the curve of spectra, for the estimation of HbA1c percentages. Calculations of the refractive index in different concentrations of Hb-glucose using Optical Coherence Tomography (OCT) were reported in [23], likewise using Abbe refractometry [14]. In [24] the authors discriminated Hb of HbA1c using the refractive index and diffraction tomography. The work [19] presents a comparison of the optical properties of HbA1c and Hb using refractometry, fluorescence, and surface enhancement Raman scattering (SERS) spectroscopy. A review in [25] presents several spectroscopic studies of the glycation of tissues and cell proteins, both in organisms showing developed diabetes naturally as well as in-vitro glycated samples, using a wide range of electromagnetic waves including optical refractometry, digital holographic microscopy, diffraction tomography, fluorescence, terahertz spectroscopy, and optical imaging.

Furthermore, the work [26] presents a model for discrimination between diabetic and non-diabetic patients, using red blood cells and Near-Infrared Raman Spectroscopy (NIRS). Authors in [19] used SERS spectroscopy to analyze the spectral behavior of lyophilized powder of human hemoglobin (Hb) and hemolysate of glycated hemoglobin (HbA1c). A procedure for the discrimination of Hb and HbA1c on both blood and commercial samplings was reported in [27], using drop-coating Raman spectroscopy (DCRS); the partial least-squares (PLS) method was applied for the calculation of the HbA1c percentage. The authors of [28] were able to characterize the spectral behavior of Hb and HbA1c using surface enhanced resonance Raman scattering

* Corresponding author.
*E-mail address:* naara@inaoep.mx (N. González-Viveros).

https://doi.org/10.1016/j.saa.2020.119077
1386-1425/

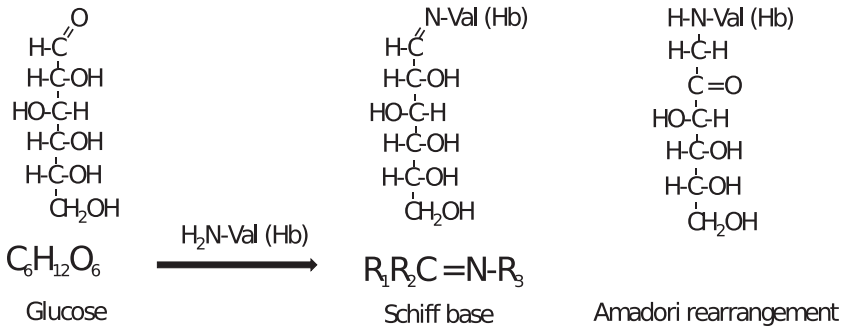


**Fig. 1.** The HbA1c formation scheme and chemical formula [6].

(SERRS) spectroscopy. The work [29] shows the feasibility of discriminating Type-II diabetic patients from non-diabetic patients, using a combination of laser tweezers and Raman spectroscopy; the authors analyzed differences in the peaks of spectra obtained from red cells of both types of patients. In [30], Hb and HbA1c Raman signals were analyzed in hemolysate of erythrocytes and in whole blood, using resonance Raman spectroscopy; the classification of HbA1c concentrations in three groups was done using a Support Vector Machine (SVM); that work includes molecular assignments of peaks.

Concerning in vivo measurement, the work [31] discriminates among diabetic and non-diabetic patients using Raman spectroscopy and SVM. The use of Terahertz spectroscopy in human skin for glucose detection was reported in [32]. The work [33] evaluated relations of advanced glycation end products in the skin using skin intrinsic

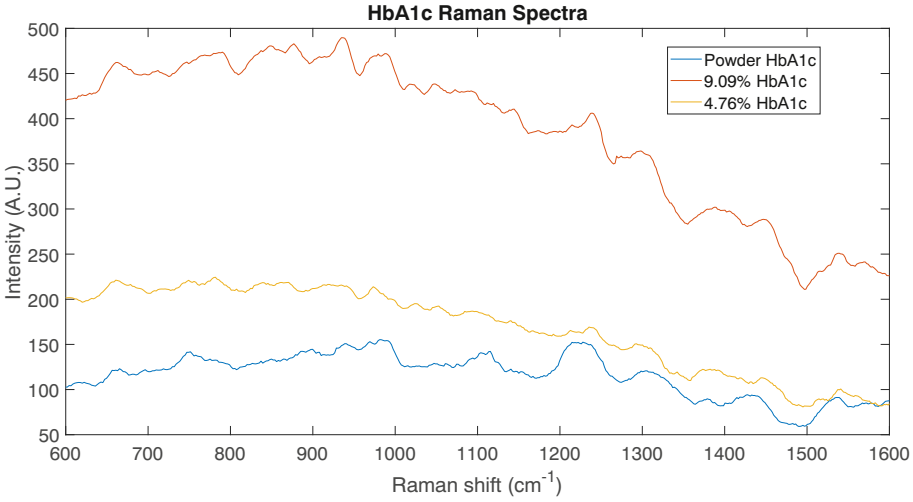


**Fig. 2.** Raman spectra of HbA1c. a) Raw spectra, b) Filtered and normalized spectra.

**Table 1**
Representative peaks and FWHM obtained from average HbA1c Raman spectra for three concentrations.

| Concentration | Raman peaks - FWHM ($cm^{-1}$) | | | | | | | | | | | | |
|---|---|---|---|---|---|---|---|---|---|---|---|---|---|
| 100% | 1578 - 42 | 1571 - 49 | 1536 - 29 | 1436 - 58 | 1311 - 53 | 1308 - 59 | 1230 - 37 | 1221 - 58 | 1114 - 15 | 1106 - 30 | 969 - 28 | 749 - 28 | 665 - 28 |
| 9.09% | 1579 - 58 | 1572 - 58 | 1542 - 12 | 1450 - 92 | 1310 - 4 | 1307 - 47 | 1238 - 35 | 1214 - 5 | 1119 - 12 | 1111 - 9 | 979 – 6 | 747 – 5 | 661 - 41 |
| 4.76% | 1579 - 55 | 1575 - 55 | 1539 - 39 | 1432 – 10 | 1315 - 49 | 1301 - 59 | 1237 - 35 | 1223 - 58 | 1113 – 5 | 1102 - 58 | 974 - 28 | 749 - 12 | 660 - 34 |

fluorescence (SIF) and multivariable regression. The authors of [34] filed a patent of an apparatus that uses FT Infrared Raman and absorbance spectrometers for the detection of glucose and HbA1c. They created a data processor to determine the percentage of glycated hemoglobin through the comparison of the extinction coefficient in a reference material. Nevertheless, no information is provided about the method for computing such approximations and no error estimation of the measurements was obtained for such apparatus.

It may be noticed that through the years, several investigations have been performed in order to achieve reliable quantification regarding the HbA1c characterization and detection. Yet, a combination of FFNN with Raman spectroscopy for the measurement of glycated hemoglobin percentages in different concentrations has not been reported. In this work, we present a spectral analysis of HbA1c commercial lyophilized sample taken in three different water-based concentrations: 100% (dry powder), 9.09%, and 4.76%. Using these data, we designed a quantitative regression model based on artificial neural networks (ANN) to estimate unknown HbA1c concentrations. Our work includes the removal of signal fluorescence through a smoothing process using a 3-point Savitzky-Golay first-order algorithm, as well as filtering and normalization of the spectra. Our experimental results showed that this methodology is a reliable estimator of both quantitative and qualitative characteristics of HbA1c at different concentrations. This analysis is a first step in the design of a non-invasive device able to estimate HbA1c concentrations in diabetic patients.

## 2. Experimental materials and methods

### 2.1. Raman spectroscopy for measurement

The characterization and analysis presented here used Raman spectroscopy measurements with an Ocean Optics Raman spectrometer QE65000, which has a resolution of 0.14–7.7 nm of Full Width at Half Maximum (FWHM) equivalent to 6 $cm^{-1}$. The experimental setup is composed of a laser source of 785 nm with a power of 10 mW, and an InPhotonics Raman probe, model RIP-RPS-785, with filtering and steering micro-optics, a numerical aperture of 0.22, and a stainless-steel cabled fiber. It is worth mentioning that the 10 mW power was obtained by coupling loss, i.e., by changing the separation between two facing fibers, making it possible to modulate the received power [35]. Measurements were taken during 10 min applying photobleaching, in order to reduce sample autofluorescence intensity [36–38]. It is important to point out that only some specific constituents of the whole HbA1c macromolecule are affected by photobleaching [39,40]. HbA1c is composed of amino acids, glucose, and other molecules [41]. A few of these amino acids such as phenylalanine, tyrosine, and tryptophan are dominant intrinsic fluorophores, therefore they are photobleaching [40,42]. On the other hand, glucose, which is not a fluorescent molecule, presents no photobleaching [39], hence the glucose intensity is not disturbed.

The HbA1c powder provided by Sigma Aldrich (ID product: IRMMIFCC466) was used to prepare the solutions. Pure powder was considered as 100% concentration; besides, two solutions were made using 10 μl and 20 μl of distilled water in which 1 mg of HbA1c was dissolved, corresponding to HbA1c concentrations of 9.09% and 4.76% respectively; these samples are similar to human concentrations [43]; ten measurements were made for each concentration. Solutions were prepared using Eq. (1) [44]; solute mass ($m_{solute}$) was set to 1 mg and water density ($\rho_{water}$) was set to 1 g/$cm^3$; water volume ($v_{water}$) was varied (10 or 20 μl).

$$\%Concentration = \frac{m_{solute}}{m_{solute} + (\rho_{water} * v_{water})} * 100 \quad (1)$$

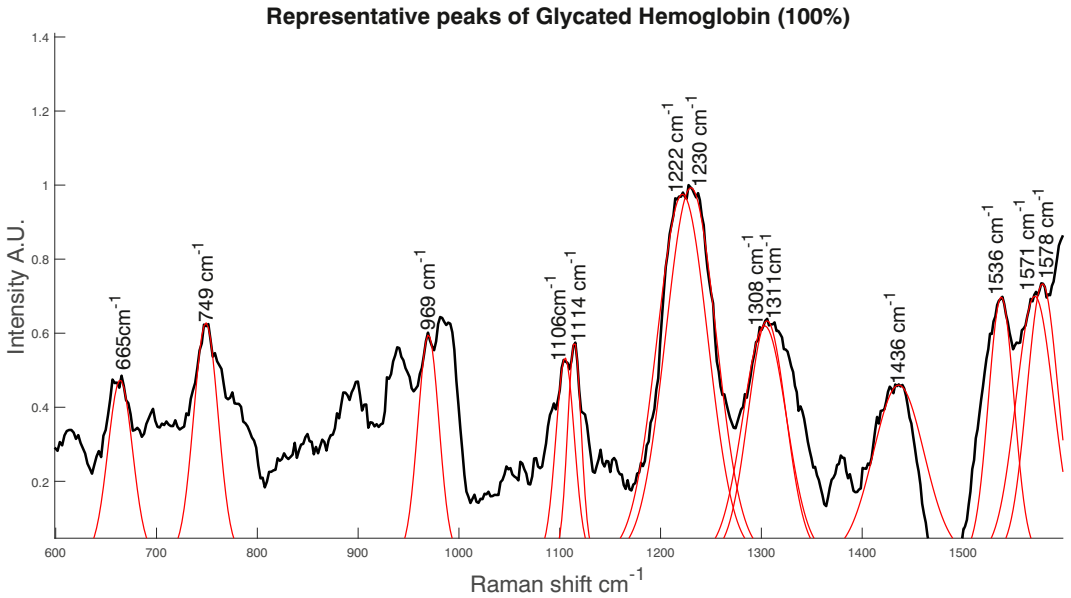


**Fig. 3.** Gaussian fit of HbA1c characteristic Raman Peaks at 100% concentration.

**Table 2**
Molecular assignment of powder HbA1c peaks, based on other works.

| Peaks positions ($cm^{-1}$) obtained in our experiments | Peaks positions ($cm^{-1}$) found in other works | Molecular assignment |
|---|---|---|
| 1578 | 1585 [67], 1582 [62,68], 1580 [64] | $\nu_{37}$ $\nu(C_\alpha C_m)_{sym}$ [62,64,67], Phenylalanine [64], $\nu_{37}$ $\nu(C_\alpha C_m)_{asym}$ [68]. |
| 1571 | 1568 [63,67] | $\nu(C_\alpha C_m)_{asym}$ [63,67] |
| 1536 | 1548 [67], 1539–1546 [65,66], 1544 [68] | Amide II ($\beta$-turn) in and out of phase combinations of C—N stretching and NH in-plane bending [65,66], $\nu(C_\beta C_\beta)$ [67], $\nu_{11}$ $\nu(C_\beta C_\beta)$ [68]. |
| 1436 | 1427 [67],1430 [68] | $\nu_{28}$ $\nu(C_\alpha C_m)_{sym}$ [67], $\nu_{28}$ $\nu(C_\alpha C_m)_{sym}$ [68]. |
| 1311 | 1310 [69] | twist [69]. |
| 1308 | 1303 [67], 1306 [68] | $\delta_{asym}(C_mH)$ [67], $\nu_{21}$ $\delta_{asym}(C_mH)$ [68]. |
| 1230 | 1228 [64], 1231 [63], 1230 [68] | $\delta(CmH)$ [64], $\nu_{13}$ [63], metRBC $\delta(C_mH)$ [68]. |
| 1222 | 1226 [67], 1222 [62], 1223–1225 [66], 1225 [68] | $\delta(C_mH)$ [62,67,68], Oxygenated state of hemoglobin, $PO_2$ asymmetric stretching vibrations, nucleic acids [66] |
| 1114 | 1120 [67], 1122–1128 [66] | $\nu_{22}$, $\delta(CH_2)$, twisting, wagging [67], C—N stretching in proteins, glucose, *C*-methyl in hemo [66]. |
| 1106 | 1106 [65] | Glucose C-O-C (bending model deformation) [65]. |
| 969 | 974 [62], 970[64], 976 [66,65], 975 [68] | $\gamma(C_aH==)$ [62], p:skeletal vibration, glutathione [64],$CH_3$ deformation [66], C—O angel-bending glucose [65], $\nu_{46}$ $\delta(\text{pyr deform})_{asym}$ [68]. |
| 749 | 755 [67], 754 [62], 753 [64,68], 754 [66] | $\nu$(pyr deform) [62], Stretching pyr. Breathing in oxyhemoglobin [64,66], $\nu$(pyr breathing) $\nu_{15}$ [68]. |
| 665 | 677 [67], 676 [64], 673 [62], 672 [66], 664 [68] | $\nu_7$ $\delta(pyrdeformation)_{sym}$ [62,64,67,68], Deoxygenated state of hemoglobin [66]. |

The SNR in Raman spectra is calculated using Eq. (2), which describes the ratio of the mean of the most intense peak $\bar{S}$ and the standard deviation at such frequency $\sigma_y$. For all the concentrations, the calculation was made using the peak at 1230 $cm^{-1}$ and ten measurements per concentration.

$$SNR = \frac{\bar{S}}{\sigma_y} \tag{2}$$

It is worth mentioning that we measured HbA1c samples at 100% (powder) applying 30 s, 40 s, and 60 s exposure time; the best SNR was 6.53, obtained using 60 s. For the same time, we obtained an SNR of 4.76 for 4.76% and 6.39 for 9.09%. Despite this being a low signal-to-noise ratio, it is enough to perform quantitative analysis as long as SNR ≥ 3 [45].

### 2.2. Fluorescence background removal

The Raman effect generates a weak intensity signal as only one out of 10,000 photons presents a shift in its frequency [46]. These signals contain several types of noise, such as shot noise, noise generated by instrumentation, noise generated by external sources (such as cosmic rays), and noise generated by sampling [47–49]. Fluorescence background, which manifests itself as a smooth curve of the baseline of the spectrum, is also considered as noise by several authors [48–51]. Indeed, fluorescence removal facilitates distinguishing the positions of the peaks and their widths [52]. There are several methods to eliminate fluorescence in Raman spectra and smoothing them [48,50,53,54]. For the experiments reported here, each Raman spectrum was pre-processed using a fifth-degree polynomial approximation function, followed by a smoothing using a 3-point Savitzky-Golay 1st order algorithm. The polynomial curve fitting builds a function using a set of data points, calculating the coefficients of a polynomial of a degree $n - 1$ [53]. The Savitzky-Golay method generates a smoothed data function that preserves the original data distribution [55].

### 2.3. Principal component analysis

Principal Component Analysis (PCA) is a technique that transforms the original set of variables into another set of new uncorrelated variables, known as the principal components (PC). The PC that provide most information on the data may be selected as inputs for building an estimation model of the concentration of HbA1c in a sample [56].

### 2.4. Regression based on artificial neural networks (ANN)

Regression-based in ANN is used in this research to approximate a relation between a dependent variable (the HbA1c value) and one or more independent variables (PC values of the Raman spectra). ANN are mathematical models that may be used for estimating the outputs of a multivariable function for a given set of inputs or regressors. There are several kinds of ANN, being feed-forward neural networks (FFNN), one of the most popular architectures for function approximation.

The architecture of an FFNN is based on elements called neurons, organized by layers, where neurons of one layer connect to the next one. Each neuron has associated with a scalar value known as a weight, which allows interaction with other neurons. The output of each neuron is calculated as the weighted addition of outputs coming from neurons in the previous layer, smoothed by a function called activation function. The value of the weights is calculated using a training algorithm, through examples of the inputs and desired outputs of the function to be estimated [57].

In this paper, an application provided by MATLAB 2019a, called Neural Net Fitting, was used for carrying out the concentration prediction using a regression. The ANN architecture is an FFNN composed of two layers, using a sigmoid activation function for neurons in the hidden layer and a pure linear function for neurons in the output layer. The Levenberg-Marquardt and Scaled Conjugate Gradient algorithms were used for training; the number of neurons in the hidden layer was chosen as a function of the network performance, measured by the Root Mean Square Error in Cross-Validation (RMSECV).

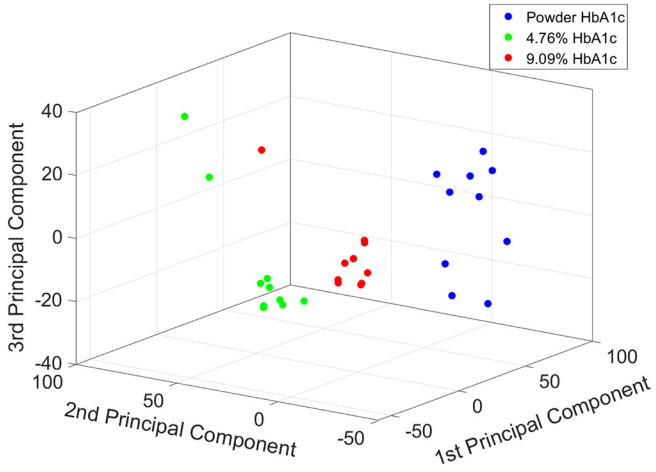


**Fig. 4.** HbA1c concentrations representation by three PC. Each point represents a sampling spectrum.

**Table 3**
Best FFNN architectures and their performance as regression models using PC obtained from two different bands of Raman spectra.

| Spectral Range | Model 1 (600–1600 $cm^{-1}$) | Model 2 (1150–1300 $cm^{-1}$) |
|---|---|---|
| Filtering Process | Polyfit and Savitzky Golay | Polyfit and Savitzky Golay |
| # hidden neurons | 5 | 6 |
| Training Algorithm | Levenberg-Marquardt backpropagation | Levenberg-Marquardt backpropagation |
| Activation Function | Hyperbolic tangent sigmoid and linear | Hyperbolic tangent sigmoid and linear |
| RMSECV | 0.54% ± 0.17 | 0.08% ± 0.04 |

## 3. Results and discussion

### 3.1. Raman spectrum analysis

Representative peaks were obtained using MATLAB's function findpeaks, which returns the local maxima (peaks) of an input signal [58]. Fig. 2 (a) shows the average of ten raw samples of HbA1c Raman spectra, with concentrations of 100%, 4.76%, and 9.09%; Fig. 2 (b) shows the average of such samples after being filtered and normalized. Note that some peaks appear in the same position for the three concentrations, while others present a shift; this is also observed in Table 1 which lists all representative peaks for the three concentrations. For example, the highest peak in Fig. 2 (b), located at 1230 $cm^{-1}$, shifts a few $cm^{-1}$ among concentrations; this behavior has been reported with other substances while diluted in water [59–61].

HbA1c is composed of sub-units of globin, α1, α2, β1 and β2; each sub-unit is stuck together by a heme group; there is glucose attached across its surface [6]. Fig. 3 shows the Raman peaks in a signal resulting from the average of ten Raman spectra, obtained from HbA1c powder (100% concentration).

Considering the heme group, Raman spectra of the HbA1c powder show vibrations of $\delta_{asym}(C_mH)$ at 1230 $cm^{-1}$; other vibrations are found at 1308 $cm^{-1}$ due to methine C—H deformation and $\nu(C_\alpha C_m)_{asym}$; the peak at 1571 $cm^{-1}$ shows a vibration of $\nu(C_\alpha C_m)_{asym}$; glucose attached to hemoglobin may produce the Raman shift at 1106 $cm^{-1}$ due to $\delta(C-O-C)$ stretching bond, the peak at 1536 $cm^{-1}$ may be assigned to Amide II by the stretching CN and CNH bending in tryptophan, of the deoxygenated state of hemoglobin [62–67]. Other peaks are present in the Raman spectra; Table 2 shows a complete list of them, compared to peak positions reported in other works.

The Raman shift observed in different concentrations (see Table 1) may also be originated from the spectrometer error, which corresponds to an FWHM ≈ 6 $cm^{-1}$; a variation of ±2 $cm^{-1}$ may be caused by the smoothing of spectra, while other sources of error may be originated from humidity, temperature changes and the water, approximately ± 2 $cm^{-1}$, according to our previous experiments.

### 3.2. Concentration analysis

Raman spectra contain the chemical information of the sample, represented by the intensity in different Raman shifts or bands. Among these, some characteristics have the same origin of variation, which results in strong correlations among a few variables in the Raman shift, which gives room for a dimensional reduction. As we stated before, we used PCA for obtaining 3 PC that represent the primary information contained in the spectrum. Fig. 4 plots the feature space of such representations for all samples involved in these experiments.

Besides, we design FFNN-based regression models to be used when the concentrations of a sample are unknown. Such models were calibrated using known values of the three concentrations; after that, they were assessed using a 5-fold cross-validation strategy.

Two regression models were built: the first one uses as input the PC obtained from the portion of the spectra going from 600 to 1600 $cm^{-1}$ [70]. The second model uses spectra located in a band running from 1150 to 1300 $cm^{-1}$; this interval was chosen because it is the region where the most intense peaks of HbA1c had been found experimentally. Our experiments have shown that the highest intensity is located at around 1230 $cm^{-1}$ with a spectral width of 37 $cm^{-1}$. Both models were designed for best performance, adjusting the number of hidden nodes and the training algorithms for the FFNN, using a training set of samples. Validation tests looking for such suitable hyper-parameters run from 5 to 20 hidden nodes, using Levenberg-Marquardt and Scaled Conjugate Gradient algorithms. A hyperbolic tangent sigmoid was used as an activation function in the hidden layer, while a linear function was used in the output layer. After finding the best combination using training data, the models were assessed using a testing set; the parameters and performance results are shown in Table 3. The best RMSECV = 0.08% ± 0.04 was obtained by the regression calibrated using data from the band containing the highest peaks, that is within 1150–1300 $cm^{-1}$.

## 4. Conclusions

In this work, we analyzed the Raman spectra generated by three different concentrations of HbA1c diluted in water. The fluorescence and noise of spectra were eliminated, and the peaks were computed using the MATLAB function find-peaks. The detected peaks show the presence of C — O — C, C — H, $C_mH$, and $C_\alpha C_m$ bonds, corresponding to Amide II characteristics of hemoglobin (heme group, α, and β chains) and glucose. Two nonlinear regression models were constructed using an FFNN based fitting procedure used when the HbA1c concentration is unknown; it is important to highlight that this adaptive regression method has not been evaluated before for commercial HbA1c substances. The model based on the band within 1150–1300 $cm^{-1}$, which contains the most intense peak found in the experiments (at 1230 $cm^{-1}$), obtained the best RMSECV of 0.08% using testing data. These results suggest the capability of Raman spectroscopy for analyzing HbA1c in different concentrations. The next step is to measure more concentrations and mixtures of Hb and HbA1c as a blood phantom. After that, we aim to design a procedure for approximating the amount of HbA1c in human blood by using neural regression, several feature extraction and selection methods, through processing and analyzing such measurements.

## Authors contributions

Conceptualization, N. G. V., J. C.R.; Formal analysis, N. G. V., J. C.R., P. G. G; Investigation, P. G. G and J. C.R.; Methodology, N. G. V. and J. C.R.; Project administration, J. C.R., P. G. G, H.H.C.N; Software, N. G. V. and P. G. G; Supervision, J. C.R.; Validation, J.C.R, H.H.C.N, P. G. G, N. G. V.; Visualization, N. G. V., P. G. G; Writing – original draft, N. G. V.; Writing – review & editing, P. G. G, H.H.C.N, J. C.R.

This research was partially supported by the Doctoral Scholarship No. 583440 provided to N. Gonzalez-Viveros by the National Council of Science and Technology (CONACYT), Mexico.

## Credit authorship contribution statement

**N. González-Viveros:** Conceptualization, Formal analysis, Methodology, Project administration, Software, Validation, Visualization, Writing - original draft. **J. Castro-Ramos:** Conceptualization, Formal analysis, Investigation, Methodology, Project administration, Supervision, Validation, Writing - review & editing. **P. Gómez-Gil:** Formal analysis, Investigation, Project administration, Software, Validation, Visualization,

Writing - review & editing. **H.H. Cerecedo-Núñez:** Project administration, Validation, Writing - review & editing.

## Declaration of competing interest

The authors declare that they have no known competing financial interests or personal relationships that could have appeared to influence the work reported in this paper.

## References


[1] World Health Organization, Use of glycated haemoglobin (HbA1c) in the diagnosis of diabetes mellitus: abbreviated report of a WHO consultation., World Health Organization 2011 (2011) 1–25.

[2] L. Liu, S. Hood, Y. Wang, R. Bezverkov, C. Dou, A. Datta, C. Yuan, Direct enzymatic assay for % HbA1c in human whole blood samples, Clin. Biochem. 41 (7–8) (2008) 576–583, https://doi.org/10.1016/j.clinbiochem.2008.01.013.

[3] H.F. Bunn, D.N. Haney, S. Kamin, K.H. Gabbay, P.M. Gallop, The biosynthesis of human hemoglobin A1c. Slow glycosylation of hemoglobin in vivo, J. Clin. Invest. 57 (6) (1976) 1652–1659, https://doi.org/10.1172/JCI108436.

[4] S.I. Sherwani, H.A. Khan, A. Ekhzaimy, A. Masood, M.K. Sakharkar, Significance of HbA1c test in diagnosis and prognosis of diabetic patients, Biomark. Insights 11 (2016) 95–104, https://doi.org/10.4137/BMI.S38440.

[5] X. Zhang, K.F. Medzihradszky, J. Cunningham, P.D. Lee, C.L. Rognerud, C.-N. Ou, P. Harmatz, H.E. Witkowska, Characterization of glycated hemoglobin in diabetic patients: usefulness of electrospray mass spectrometry in monitoring the extent and distribution of glycation, J. Chromatogr. B Biomed. Sci. Appl. 759 (1) (2001) 1–15, https://doi.org/10.1016/S0378-4347(01)00196-7.

[6] Biologic Models, Glycated hemoglobin HbA1c, visited on 05-10-2019. URL https://biologicmodels.com/project/glycated-hemoglobin-hba1c/.

[7] S.H. Ang, M. Rambeli, T.M. Thevarajah, Y.B. Alias, S.M. Khor, Quantitative, single-step dual measurement of hemoglobin A1c and total hemoglobin in human whole blood using a gold sandwich immunochromatographic assay for personalized medicine, Biosens. Bioelectron. 78 (2016) 187–193, https://doi.org/10.1016/j.bios.2015.11.045.

[8] S.H. Ang, T.M. Thevarajah, P.M. Woi, Y.B. Alias, S.M. Khor, A lateral flow immunosensor for direct, sensitive, and highly selective detection of hemoglobin A1c in whole blood, J. Chromatogr. B 1015-1016 (2016) 157–165, https://doi.org/10.1016/j.jchromb.2016.01.059.

[9] H. Sifen, P. Laitinen, U. Turpeinen, P. Karppinen, Direct monitoring of glycohemoglobin $A_{1c}$ in the blood samples of diabetic patients by capillary electrophoresis: comparison with an immunoassay method, J. Chromatogr. A 979 (1) (2002) 201–207, https://doi.org/10.1016/S0021-9673(02)01403-6.

[10] E. del Castillo, M. Montes-Bayón, E. Añón, A. Sanz-Medel, Quantitative targeted biomarker assay for glycated haemoglobin by multidimensional LC using mass spectrometric detection, Journal of Proteomics 74 (1) (2011) 35–43, doi:https://doi.org/10.1016/j.jprot.2010.07.011.

[11] S.-C. Lee, L.-H. Wang, S.-M. Tsai, H.-Y. Fang, L.-Y. Tsai, Effects of the Hb E, Hb H and Hb G-Taichung variants on HbA1c values by the Bio-Rad variant II turbo analyzer, Clin. Biochem. 44 (16) (2011) 1338–1342, https://doi.org/10.1016/j.clinbiochem.2011.08.907.

[12] M. Adamczyk, Y.-Y. Chen, D.D. Johnson, P.G. Mattingly, J.A. Moore, Y. Pan, R.E. Reddy, Chemiluminescent acridinium-9-carboxamide boronic acid probes: application to a homogeneous glycated hemoglobin assay, Bioorg. Med. Chem. Lett. 16 (5) (2006) 1324–1328, https://doi.org/10.1016/j.bmcl.2005.11.062.

[13] K. Hirokawa, K. Nakamura, N. Kajiyama, Enzymes used for the determination of $HbA_{1c}$, FEMS Microbiol. Lett. 235 (1) (2004) 157–162, https://doi.org/10.1111/j.1574-6968.2004.tb09581.x.

[14] O.S. Zhernovaya, V.V. Tuchin, I.V. Meglinski, Monitoring of blood proteins glycation by refractive index and spectral measurements, Laser Phys. Lett. 5 (6) (2008) 460–464, https://doi.org/10.1002/lapl.200810007.

[15] M. Beatriz de la Calle Guntiñas, R. Wissiack, G. Bordin, A. R. Rodríguez, Determination of haemoglobin $A_{1c}$ by liquid chromatography using a new cation-exchange column, Journal of Chromatography B 791 (1) (2003) 73–83, doi:https://doi.org/10.1016/S1570-0232(03)00202-2.

[16] A. Maleska, C. Hirtz, E. Casteleyn, O. Villard, J. Ducos, A. Avignon, A. Sultan, S. Lehmann, Comparison of HbA1c detection in whole blood and dried blood spots using an automated ion-exchange HPLC system, Bioanalysis 9 (5) (2017) 427–434, https://doi.org/10.4155/bio-2016-0278.

[17] Y. Li, J.O. Jeppsson, M. Jörntén-Karlsson, E. Linné Larsson, H. Jungvid, I.Y. Galaev, B. Mattiasson, Application of shielding boronate affinity chromatography in the study of the glycation pattern of haemoglobin, J. Chromatogr. B 776 (2) (2002) 149–160, https://doi.org/10.1016/S1570-0232(02)00162-9.

[18] M. Thevarajah, M.N. Nadzimah, Y.Y. Chew, Interference of hemoglobinA1c (HbA1c) detection using ion-exchange high performance liquid chromatography (HPLC) method by clinically silent hemoglobin variant in University Malaya Medical Centre (UMMC)—a case report, Clin. Biochem. 42 (4) (2009) 430–434, https://doi.org/10.1016/j.clinbiochem.2008.10.015.

[19] E.N. Lazareva, A.Y. Zyubin, I.G. Samusev, V.A. Slezhkin, V.I. Kochubey, V.V. Tuchin, Refraction, fluorescence, and Raman spectroscopy of normal and glycated hemoglobin, in: Biophotonics: Photonic Solutions for Better Health Care VI, vol. 10685, International Society for Optics and Photonics, SPIE, 2018 636–643, https://doi.org/10.1117/12.2307102.

[20] R. Pandey, N.C. Dingari, N. Spegazzini, R.R. Dasari, G.L. Horowitz, I. Barman, Emerging trends in optical sensing of glycemic markers for diabetes monitoring, TrAC Trends Anal. Chem. 64 (2015) 100–108, https://doi.org/10.1016/j.trac.2014.09.005.

[21] R. Pandey, Raman spectroscopy-based sensing of glycated hemoglobin: critical analysis and future outlook, Journal of Postdoctoral Research 3 (2) (2015) 8–16. URL http://www.postdocjournal.com/file_journal/766_23669297.pdf.

[22] M. Mallya, R. Shenoy, G. Kodyalamoole, M. Biswas, J. Karumathil, S. Kamath, Absorption spectroscopy for the estimation of glycated hemoglobin (HbA1c) for the diagnosis and management of diabetes mellitus: a pilot study, Photomed. Laser Surg. 31 (5) (2013) 219–224, https://doi.org/10.1089/pho.2012.3421.

[23] O.S. Zhernovaya, A.N. Bashkatov, E.A. Genina, V.V. Tuchin, I.V. Meglinski, D.Y. Churmakov, L.J. Ritchie, Investigation of glucose- hemoglobin interaction by optical coherence tomography, in: V.V. Tuchin (Ed.), Saratov Fall Meeting 2006: Optical Technologies in Biophysics and Medicine VIII, vol. 6535, SPIE, International Society for Optics and Photonics 2007, pp. 423–429, https://doi.org/10.1117/12.740985.

[24] G. Mazarevica, T. Freivalds, A. Jurka, Properties of erythrocyte light refraction in diabetic patients, J. Biomed. Opt. 7 (2) (2002) 244–247, https://doi.org/10.1117/1.1463043.

[25] O.A. Smolyanskaya, E.N. Lazareva, S.S. Nalegaev, N.V. Petrov, K.I. Zaytsev, P.A. Timoshina, D.K. Tuchina, Y.G. Toropova, O.V. Kornyushin, A.Y. Babenko, J.-P. Guillet, V.V. Tuchin, Multimodal optical diagnostics of glycated biological tissues, Biochem. Mosc. 84 (1) (2019) 124–143, https://doi.org/10.1134/S0006297919140086.

[26] T. Pan, M. Li, J. Chen, H. Xue, Quantification of glycated hemoglobin indicator HbA1c through near-infrared spectroscopy, Journal of Innovative Optical Health Sciences 07 (4) (2014) 1350060, https://doi.org/10.1142/S1793545813500600.

[27] I. Barman, N.C. Dingari, J.W. Kang, G.L. Horowitz, R.R. Dasari, M.S. Feld, Raman spectroscopy-based sensitive and specific detection of glycated hemoglobin, Anal. Chem. 84 (5) (2012) 2474–2482, https://doi.org/10.1021/ac203266a.

[28] M. Syamala Kiran, T. Itoh, K.-i. Yoshida, N. Kawashima, V. Biju, M. Ishikawa, Selective detection of HbA1c using surface enhanced resonance Raman spectroscopy, Anal. Chem. 82 (4) (2010) 1342–1348, https://doi.org/10.1021/ac902364h.

[29] J. Lin, L. Shao, S. Qiu, X. Huang, M. Liu, Z. Zheng, D. Lin, Y. Xu, Z. Li, Y. Lin, R. Chen, S. Feng, Application of a near-infrared laser tweezers Raman spectroscopy system for label-free analysis and differentiation of diabetic red blood cells, Biomed. Opt. Express 9 (3) (2018) 984–993, https://doi.org/10.1364/BOE.9.000984.

[30] R. Pandey, S.P. Singh, C. Zhang, G.L. Horowitz, N. Lue, L. Galindo, R.R. Dasari, I. Barman, Label-free spectrochemical probe for determination of hemoglobin glycation in clinical blood samples, J. Biophotonics 11 (10) (2018), e201700397, https://doi.org/10.1002/jbio.201700397.

[31] J.F. Villa-Manríquez, J. Castro-Ramos, F. Gutiérrez-Delgado, M.A. Lopéz-Pacheco, A.E. Villanueva-Luna, Raman spectroscopy and PCA- SVM as a non-invasive diagnostic tool to identify and classify qualitatively glycated hemoglobin levels in vivo, J. Biophotonics 10 (8) (2017) 1074–1079, https://doi.org/10.1002/jbio.201600169.

[32] O. Cherkasova, M. Nazarov, A. Shkurinov, Noninvasive blood glucose monitoring in the terahertz frequency range, Opt. Quant. Electron. 48 (3) (2016) 217, https://doi.org/10.1007/s11082-016-0490-5.

[33] D.L. Felipe, J.M. Hempe, S. Liu, N. Matter, J. Maynard, C. Linares, S.A. Chalew, Skin intrinsic fluorescence is associated with hemoglobin $A_{1c}$ and hemoglobin glycation index but not mean blood glucose in children with type 1 diabetes, Diabetes Care 34 (8) (2011) 1816–1820, https://doi.org/10.2337/dc11-0049.

[34] S. Kim, J. Lee, Noninvasive apparatus and method for testing glycated hemoglobin, visited on 30-12-2019 (March 2016). URL https://patents.google.com/patent/US20160061810A1/en.

[35] D. Tosi, G. Perrone, Optical Fiber Sensors for Biomedical Applications, Artech House 2017.

[36] P. Lemler, W.R. Premasiri, A. Delmonaco, L.D. Ziegler, NIR Raman spectra of whole human blood: effects of laser-induced and in vitro hemoglobin denaturation, Anal. Bioanal. Chem. 406 (1) (2014) 193–200, https://doi.org/10.1007/s00216-013-7427-7.

[37] D. Cebeci-Maltaş, D. Ben-Amotz, M.A. Alam, P. Wang, R. Pinal, Photobleaching profile of Raman peaks and fluorescence background, European Pharmaceutical Review 22 (6) (2017) 18–21https://www.europeanpharmaceuticalreview.com/article/70503/raman-peaks-fluorescence-background/.

[38] I. Barman, C.-R. Kong, G.P. Singh, R.R. Dasari, Effect of photobleaching on calibration model development in biological Raman spectroscopy, J. Biomed. Opt. 16 (1) (2011) 1–10, https://doi.org/10.1117/1.3520131.

[39] D.C. Klonoff, Overview of fluorescence glucose sensing: a technology with a bright future, J. Diabetes Sci. Technol. 6 (6) (2012) 1242–1250, https://doi.org/10.1177/193229681200600602.

[40] J. R. Lakowicz, Protein fluorescence., in: Principles of Fluorescence Spectroscopy, Springer, 2006, pp. 529–575, doi:https://doi.org/10.1007/978-0-387-46312-4_16.

[41] A. Blanco, G. Blanco, Chapter 3 - proteins, in: A. Blanco, G. Blanco (Eds.), Medical Biochemistry, Academic Press, 2017, pp. 21–71, doi:https://doi.org/10.1016/B978-0-12-803550-4.00003-3.

[42] R. E. Hirstch, Hemoglobin fluorescence, Humana Press, Totowa, NJ, 2003, pp. 133–154, doi:-443.webvpn.fjmu.edu.cn/10.1385/1-59259-373-9:133 .

[43] C. Weykamp, HbA1c: a review of analytical and clinical aspects, Ann. Lab. Med. 33 (6) (2013) 393–400, https://doi.org/10.3343/alm.2013.33.6.393.

[44] P. Flowers, K. Theopold, R. Langley, W.R. Robinson, Chemistry 2e, Open-Stax 2015.

[45] L. Richard, McCreery, Raman Spectroscopy for Chemical Analysis, John Wiley & Sons, Inc., 2000

[46] G.R. Desiraju, The Raman effect, Nature India (2008) 1–3, https://doi.org/10.1038/nindia.2008.302.

[47] M. J. Pelletier, C. C. Pelletier, Spectroscopic theory for chemical imaging, John Wiley & Sons, Ltd, 2011, Ch. 1, pp. 1–20, doi:https://doi.org/10.1002/9780470768150.ch1.

[48] J. Smulko, M. S. Wróbel, Noise sources in Raman spectroscopy of biological objects, in: Dynamics and Fluctuations in Biomedical Photonics XIV, Vol. vol. 10063, International Society for Optics and Photonics, SPIE, 2017, pp. 54–60, doi:https://doi.org/10.1117/12.2254807.

[49] J.M. Smulko, N.C. Dingari, J.S. Soares, I. Barman, Anatomy of noise in quantitative biological Raman spectroscopy, Bioanalysis 6 (3) (2014) 411–421, https://doi.org/10.4155/bio.13.33724471960.

[50] A. E. Villanueva-Luna, Espectroscopia Raman en fluidos biol'ogicos extracelulares [Raman Spectroscopy in extra-cellular biological fluids], Phd thesis, Instituto Nacional de Astrofisica Óptica y Electr'onica (2013).

[51] T. Yamanaka, H. Nakagawa, M. Ochida, S. Tsubouchi, Y. Domi, T. Doi, T. Abe, Z. Ogumi, Ultrafine fiber Raman probe with high spatial resolution and fluorescence noise reduction, J. Phys. Chem. C 120 (2016) 2585–2591, https://doi.org/10.1021/acs.jpcc.5b11894.

[52] J. M. Shaver, Chemometrics for Raman spectroscopy, in: I. R. Lewis, H. G. M. Edwards (Eds.), Handbook of Raman Spectroscopy: From the Research Laboratory to the Process Line, Taylor & Francis Group, New York, 2001, Ch. 7.

[53] E. W. Weisstein, Least squares fitting–polynomial, visited on 2019-01-17. URL https://mathworld.wolfram.com/LeastSquaresFittingPolynomial.html.

[54] S.J. Barton, T.E. Ward, B.M. Hennelly, Algorithm for optimal denoising of Raman spectra, Anal. Methods 10 (30) (2018) 3759–3769, https://doi.org/10.1039/C8AY01089G.

[55] A. Savitzky, M.J.E. Golay, Smoothing and differentiation of data by simplified least squares procedures, Anal. Chem. 36 (8) (1964) 1627–1639, https://doi.org/10.1021/ac60214a047.

[56] R. Bro, A. K. Smilde, Principal component analysis, Anal. Methods 6 (2014) 2812–283, doi:https://doi.org/10.1039/C3AY41907J.

[57] S. Haykin, Neural Networks and Learning Machines, 3rd Edition, Prentice Hall 2009.

[58] MathWorks, Findpeaks: Find local maxima, visited on 2019-09-01. URL https://es.mathworks.com/help/signal/ref/findpeaks.html.

[59] I. Halasz, M. Agarwal, R. Li, N. Miller, Vibrational spectra and dissociation of aqueous $Na_2SiO_3$ solutions, Catal. Lett. 117 (2007) 34–42, https://doi.org/10.1007/s10562-007-9141-6.

[60] M. S. Bradley, Lineshapes in IR and Raman spectroscopy: a primer, Spectroscopy 30 (11) (2015) 42–46. URL https://www.spectroscopyonline.com/view/lineshapes-ir-and-raman-spectroscopy-primer.

[61] H. Vašková, M. Toměcek, Rapid spectroscopic measurement of methanol in water-ethanol-methanol mixtures, MATEC Web Conf. 210 (2018) 02035, doi:https://doi.org/10.1051/matecconf/201821002035.

[62] C.G. Atkins, K. Buckley, M.W. Blades, R.F.B. Turner, Raman spectroscopy of blood and blood components, Appl. Spectrosc. 71 (5) (2017) 767–793, https://doi.org/10.1177/0003702816686593.

[63] H. Sato, H. Chiba, H. Tashiro, Y. Ozaki, Excitation wavelength-dependent changes in Raman spectra of whole blood and hemoglobin: comparison of the spectra with 514.5-, 720- , and 1064-nm excitation, Journal of Biomedical Optics 6 (3) (2001) 366–370, doi:https://doi.org/10.1117/1.1380668.

[64] J. Lin, J. Lin, Z. Huang, P. Lu, J. Wang, X. Wang, R. Chen, Raman spectroscopy of human hemoglobin for diabetes detection, Journal of Innovative Optical Health Sciences 07 (01) (2014) 1350051, https://doi.org/10.1142/S179354581350051X.

[65] I. H. Boyaci, H. T. Temiz, H. E. Geniş, E. Acar Soykut, N. N. Yazgan, B. Güven, R. S. Uysal, A. G. Bozkurt, K. İlaslan, O. Torun, F. C. Dudak Şeker, Dispersive and FT-Raman spectroscopic methods in food analysis, RSC Adv. 5 (70) (2015) 56606–56624, doi:https://doi.org/10.1039/C4RA12463D.

[66] T. Makhnii, O. Ilchenko, A. Reynt, Y. Pilgun, A. Kutsyk, D. Krasnenkov, M. Ivasyuk, V. Kukharskyy, Age-related changes in FTIR and Raman spectra of human blood, Ukrainian Journal of Physics 61 (10) (2016) 853–862, doi:10.15407/ujpe61.10.0853 .

[67] X. Qiu, H. Huang, Z. Huang, Z. Zhuang, Z. Guo, S. Liu, Effect of red light-emitting diodes irradiation on hemoglobin for potential hypertension treatment based on confocal micro-Raman spectroscopy, Scanning 5067867 (2017)https://doi.org/10.1155/2017/5067867.

[68] B. R. Wood, B. Tait, D. McNaughton, Micro-Raman characterisation of the R to T state transition of haemoglobin within a single living erythrocyte, Biochimica et Biophysica Acta (BBA) - Molecular Cell Research 1539 (1) (2001) 58–70, doi:https://doi.org/10.1016/S0167-4889(01)00089-1.

[69] A.M. Pawlak, J.R. Beattie, J.V. Glenn, A.W. Stitt, J.J. McGarvey, Raman spectroscopy of advanced glycation end products (AGEs), possible markers for progressive retinal dysfunction, J. Raman Spectrosc. 39 (11) (2008) 1635–1642, https://doi.org/10.1002/jrs.2011.

[70] E. Guevara, J. C. Torres-Galván, M. G. Rańırez-EÍıas, C. Luevano-Contreras, F. J. González, Use of Raman spectroscopy to screen diabetes mellitus with machine learning tools, Biomed. Opt. Express 9 (10) (2018) 4998–5010, doi:https://doi.org/10.1364/BOE.9.004998.